Int J Mater Form (2009) Vol. 2 Suppl 1:559–562
DOI 10.1007/s12289-009-0427-7

ON THE PERFORMANCE OF SUBSTRUCTURING IMPLICIT SIMULATION OF SINGLE POINT INCREMENTAL FORMING

A. Hadoush[1]*, **A. H. van den Boogaard**[2]

[1] Materials Innovation Institute
[2] Faculty of Engineering and Technology, University of Twente

ABSTRACT: This paper investigates the computational performance of the direct substructuring method. Substructuring is used to reduce the computing time in the implicit simulation of single point incremental forming (SPIF). Substructuring divides the finite element (FE) mesh into several non-overlapped substructures. The substructures are categorized into two groups: the plastic–nonlinear–substructures and the elastic–pseudo-linear–substructures. The plastic substructures assemble a part of the FE mesh that is in contact with the forming tool; they are treated by the fully nonlinear method. The elastic substructures model the elastic deformation of the rest of the FE mesh. Two approaches are used to treat the elastic substructures: the linearized approach and the condensed linearized approach. In both approaches, the geometrical and the material behaviour are assumed linear within the increment. The geometrical and material nonlinearity are considered after convergence. Combined with the plastic substructures treatment, the approaches are refered to as the plastic linear elastic (PLE) approach and the plastic condensed linear elastic approach (PCLE). The substructures categorization in plastic and elastic substructures is adapted during the simulation to capture the tool motion. Different sizes for the substructures are considered. In an example of 1600 shell elements, the best results achieved by the PLE speeding–up the classical implicit simulation by 2.82 times.

KEYWORDS: Substructuring, Incremental forming, Finite element

1 INTRODUCTION

Single Point Incremental Forming (SPIF) is a displacement controlled process performed on a CNC machine. A clamped blank is deformed by the movement of the tool that follows a prescribed tool path [1], a sketch of SPIF is presented in Figure 1. Because SPIF is a dieless process, it is perfectly suited for prototyping and small volume production. The simulation of SPIF results in enormous computing times for two reasons. First of all, the blank is deformed by a sequence of small increments that requires thousands of numerical increments to be performed. Secondly, the small contact area between the forming tool and the blank requires a very fine FE mesh to capture the introduced deformation. The extreme computing times currently limit the applicability of FE simulations to very simple academic samples.

The implicit simulation of SPIF provides a very good agreement with experimental data [2]. For nonlinear implicit simulations, the Newton–Raphson method is often preferred because of its quadratic convergence behaviour but every iteration is relatively expensive. The modified Newton–Raphson method is cheaper per iteration, but it shows only linear convergence behaviour [3]. In SPIF simulation, it has been noticed that the over all computing time by a modified Newton–Raphson method is higher than the computing time by a full Newton–Raphson method, because it requires much more iterations per increment to converge.

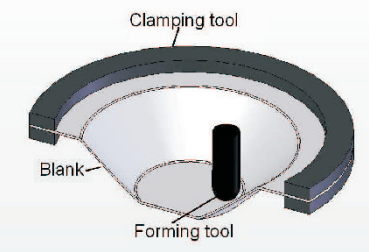

Figure 1: *Schematic representation of the SPIF process.*

The deformation in SPIF is modeled as localized plastic deformation [4]. According to this hypothesis plastic deformation is localized in a small zone in the region of the forming tool surrounded by elastic deformation of the rest of the blank. The localized plastic deformation results in a localized nonlinearity in the FE mesh. The contribution of this paper is to treat the localized plastic part of the blank by a full Newton–Raphson iterative procedure, while the non-localized deformation is modeled by a linearized elastic predictor and corrector that is updated every increment. This is implemented by substructuring. It is used as tool to manage the assembly of the predictor and the corrector. This approach combines the advantage of a

*Corresponding author: Materials Innovation Institute, P.O. Box 5008, 2600 GA Delft, The Netherlands, +31 53 489 4567, a.hadoush@m2i.nl

fast convergence for the highly nonlinear process in the plastic part with a cheap calculation in the much larger elastic part of the blank, significantly reducing the total computing time. For the linearized elastic predictor and corrector, static condensation is considered as an option in order to reduce the size of the SOEs. Similar approaches have been introduced in computational mechanics and two of them are mentioned here. The first approach is the subcycling in explicit methods to overcome the problem of very small or very stiff elements [5]. The second approach is the implicit-explicit method, where part of the system Jacobian matrix is treated implicitly and part explicitly [6].

In this paper, two different approaches are introduced to implement substructing in the implicit scheme, The approaches are the plastic linear elastic (PLE) approach and the plastic condensed linear elastic (PCLE) approach. A simple academic simulation is presented. As effeciency measure, the required computing time of the approaches are compared to the computing time for the standard fully nonlinear iterative implicit (Standard) method, as a reference.

2 SUBSTRUCTURING

Direct substructuring is considered as a non-overlapping domain decomposition method. It is a way to organise the static condensation of large linear systems arising from the discretization of partial differential equations [7]. In this section, the implicit solution of the nonlinear SOE is substructured in order to manage the calculation of predictor and corrector and performing the stress update for SPIF simulation. In the iterative procedure, the Newton–Raphson method updates an incremental displacement vector d with an iterative displacement vector Δd, using the tangent of the nonlinear SOEs $A(d)$ or in engineering terms the effective tangent stiffness matrix, by solving

$$r_{\mathrm{j}+1}(d) = r_{\mathrm{j}}(d) + A_{\mathrm{j}}(d)\Delta d_{\mathrm{j}} = 0 \tag{1}$$

where the residual $r(d)$ defines the difference between the internal forces and the external forces. The subscript j is the iteration number. Substructuring divides the FE mesh into substructures. For each substructure the linearized model in equation (1) becomes

$$\begin{pmatrix} r_i \\ r_e \end{pmatrix}^s_{j+1} = \begin{pmatrix} r_i \\ r_e \end{pmatrix}^s_j + \begin{bmatrix} A_{ii} & A_{ie} \\ A_{ei} & A_{ee} \end{bmatrix}^s_j \begin{pmatrix} \Delta d_i \\ \Delta d_e \end{pmatrix}^s \tag{2}$$

The subscripts i and e represent internal and external DOFs respectively. The superscript s refers to substructure number, $s = 1, 2, ..., n$ where n is the total number of substructures in the FE model.

According to the localized plastic deformation hypothesis in SPIF, the plastic deformation is localized in a small zone in the region of the forming tool surrounded by elastic deformation of the rest of the blank. For that reason, the substructures are categorized into plastic substructures and elastic substructures. The plastic substructures model the introduced plastic deformation in the blank by the forming tool. On the other hand, the elastic substructures model the elastic deformation of the rest of the blank. The plastic substructures are treated by the fully nonlinear method. For the elastic substructures, two approaches are introduced. The first approach is to assume a linear geometrical and material behaviour with the increment. The geometrical and material nonlinearity are considered after the convergence of the increment. This approach combined with plastic treatment of the plastic substructures will be refered to as the plastic linear elastic (PLE) approach. The second approach is to use a condensed linear geometrical and material behaviour within the increment and to consider the nonlinearity after the convergence. Comabined with the plastic substrctures treatment is called the plastic condensed linear elastic (PCLE) approach.

2.1 PLE APPROACH

The plastic substructures are iteratively treated by fully nonlinear method. For elastic substructures, the effective tangent stiffness matrix A^s and the residual r^s contains only the contribution of the internal force since there is no external force. At the beginning of each increment, A^s and r^s are calculated. A^s is kept constant during the iterative procedure. Linearly, r^s is updated by the multiplication of A^s and the incremental displacement d

$$\begin{pmatrix} r_i \\ r_e \end{pmatrix}^s_j = \begin{pmatrix} r_i \\ r_e \end{pmatrix}^s_0 + \begin{bmatrix} A_{ii} & A_{ie} \\ A_{ei} & A_{ee} \end{bmatrix}^s_0 \begin{pmatrix} d_i \\ d_e \end{pmatrix}^s \tag{3}$$

The global SOE is assembled from the contributions of the plastic substructures and the elastic substructures. The global SOE is solved for Δd. After convergence, the nonlinear stress update is performed for the elastic substructures. The main advantage of this approach is that the calculation of A^s and the stress update is performed only once per increment for the elastic substructures combined with a linear update for the r^s. This saves the redundant computing time of calculating those values iteratively.

2.2 PCLE APPROACH

Beside the plastic–elastic substructural treatment in the PLE approach, condensation is implemented for the elastic substructures. After the calculation of A^s and r^s, the internal (slave) DOFs contribution in the substructural linearized model are statically condensed to the external (master) DOFs

$$\Delta d^s_i = (A^s_{ii,0})^{-1}(-r^s_{i,0} - A^s_{ie,0}\Delta d^s_e) \tag{4}$$

that reduces the substructural linearized model to

$$r^s_{c,j+1} = r^s_{c,j} + A^s_{c,0}\Delta d^s_e \tag{5}$$

where

$$A^s_{c,0} = A^s_{ee,0} - A^s_{ei,0}(A^s_{ii,0})^{-1}A^s_{ie,0} \tag{6}$$

The substructural condensed residual $r^s_{c,j}$ is updated linearly by

$$r^s_{c,j} = r^s_{c,0} + A^s_{c,0}d^s_e \tag{7}$$

where

$$r^s_{c,0} = r^s_{e,0} - A^s_{ei,0}(A^s_{ii,0})^{-1} r^s_{i,0} \quad (8)$$

The reduced SOEs is formed by the assembly of the plastic substructures contribution and the condensed elastic substructures contribution. The reduced SOEs is solved. At the convergence of the increment, the evaluation of the internal DOFs followed by the nonlinear stress update for the elastic substructures are performed. Beside the advantage of the PLE approach, PLCE reduces the size of the SOEs significantly. On the other hand, the reduced SOEs is denser than the initial SOEs.

The PLE and the PCLE alogrithms run on a single processor. It is important to mention that the condensation, the evaluation of the internal DOFs of each substructure, the nonlinear stress update and the calculation of A^s can be done independently of the other substructures. The PCLE and The PLE algorithms can be modified to make use of parallel computing, but that is not the focus of this paper.

3 CASE STUDY

To compare the accuracy and efficiency of PLE approach and PCLE approach to the Standard approach, a single point incremental forming process of a 45° pyramidal shape is simulated with the different approaches. The 20 mm deep pyramid is made out of a $100 \times 100 \times 1.2$ mm initially flat blank. An analytical spherical tool of 10 mm radius is used. The tool follows a counter clockwise tool path for 40 loops. In each loop, the tool moves 0.5 mm vertically downwards. At a fixed vertical position, the tool performs the in-plane tool path. the simulation finishes when the tool reaches the end of loop 40. The blank edges are completely suppressed for the entire simulation. Two different substructure sizes are used. The substructure sizes are 10 mm and 20 mm ($S10$ and $S20$). For each approach two simulations are performed, one per substructure size. The total computing time of each simulation is compared to the computing time required by the Standard Newton–Raphson simulation, as reference. Each simulation is performed on one core of a Sun Fire X4450 server with Intel Xeon X5365 3 GHz processors.

3.1 ELASTIC–PLASTIC DISTRIBUTION

The considered FE mesh is divided into equal sized substructures. In Figure 2 the substructures are visualized with thick lines. A number of virtual cross points are introduced in the FE mesh. The cross point is a common node between 4 adjacent substructures. Each substructure is attached to at least one cross point. The closest cross point to the tool center categorizes the adjacent substructures as plastic substructures while the rest of the substructures are categorized as elastic substructures. The movement of the tool changes the active cross point and as result the elastic–plastic substructures distribution.

3.2 FE MODEL

The numerical blank is discretized with 1600 triangular shell elements. The element type is the discrete shear tri-

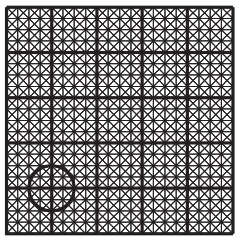

Figure 2: *Substructuring 1600 triangular element into 25 substructures, the 4 substructures in the vicinity of the tool (the circle) are plastic substructures and the others are elastic substructures.*

angle DST for bending, combined with a linear membrane element. The element has 6 DOFs per node. It has 3 integration points in plane and 5 in thickness direction (total 15). The elements are grouped for $S10$ and $S20$ in 100 substructures (with 81 virtual cross points) and 25 substructures (with 16 virtual cross points), respectively. The virtual cross points are used to determine the elastic-plastic substructure distribution. In order to focus on the substructuring technique only, the material model is kept as simple as possible. The isotropic yield behaviour of the material is modelled with the von Mises criterion. The work hardening is governed by the Swift relation:

$$\sigma = 500(\varepsilon + 0.00243)^{0.2} \quad (9)$$

Where σ and ε are the flow stress and the equivalent plastic strain, respectively. The material has a Youngs modulus of 200 GPa and Poissons ratio of 0.3. For realistic calculation, the authors acknowledge that a better material model is required, that includes the anisotropic behavior of the sheet and the cyclic mode of deformation.

3.3 RESULTS AND DISCUSSION

The Standard approach requires 6.73 hrs to finish the simulation. A speed factor is defined to compare the performance of the approaches with different substructure sizes. It is the ratio of the computing time of the Standard simulation to the considered simulation computing time. It should be larger than 1, the larger speed factor is the better in speeding the Standard approach. The simulations speed factor are summarized in Table 1. Considering the PLE approach, $S10$ simulation requires 2.38 hrs while $S20$ requires 2.99 hrs. The only difference between the Standard, $S10$ and $S20$ simulations is the total number of elements that are treated iteratively. The Standard simulation treats all elements in the FE model (1600 elements) while $S10$ and $S20$ simulations treat 64 elements and 256 elements, respectively. This results in a higher Speed factor for $S10$ (2.82) than the speed factor for $S20$ (2.25). In view of the PLCE approach, $S10$ simulation requires 2.95 hrs while $S20$ simulation requires 6.37 hrs. The speed factor of $S10$ (2.28) is higher than $S20$ (1.06), because of the condensation of a large substructural SOEs requires more time than a small substructural SOEs. Incrementally, $S20$ condenses 246 DOFs into 96 DOFs while $S10$ condenses 78 DOFs

Table 1: *The simulations Speed factor*

	Standard	PLE	PCLE
$S10$	1.0	2.82	2.28
$S20$	1.0	2.25	1.06

into only 48 DOFs. Also $S20$ treats larger number of elements than $S10$. These facts result in larger incremental cost for $S20$ than $S10$ and as a consequence a lower Speed factor. In this academic simulation, the PLE approach is more efficient reducing the total computing time for the standard simulation, for both substructural sizes $S10$ and $S20$, than PCLE for two reasons. First of all, PCLE has additional cost to the increment by the condensation. Secondly, the cost of solving the initial SOEs is almost negligible compared to iteration cost (5.3%). For this reason, the reduction in the cost of the solver has no pronounced influence in reducing the incremental cost. But for large (real life product) simulation when solver time becomes problematic, it will have more contribution in reducing the incremental cost. It is currently investigated.

In Figure 3 the results obtained by the Standard, PLE ($S10$) and PCLE ($S10$) simulations are presented. Both PLE and PCLE results show a very good agreement with the Standard results. The achieved vertical displacement (left) maximum value is 19.95 mm for the Standard simulation while PLE and PCLE have less than 0.05% error in the maximum value. The maximum equivalent plastic strain for the highest plane of integration points (right) is 0.855. The same value is achieved by the PLE and PCLE simulations with almost equal contour distribution compared to the Standard simulation contour distribution. $S20$ results have the same good agreement with the Standard results, for Both PLE and PCLE.

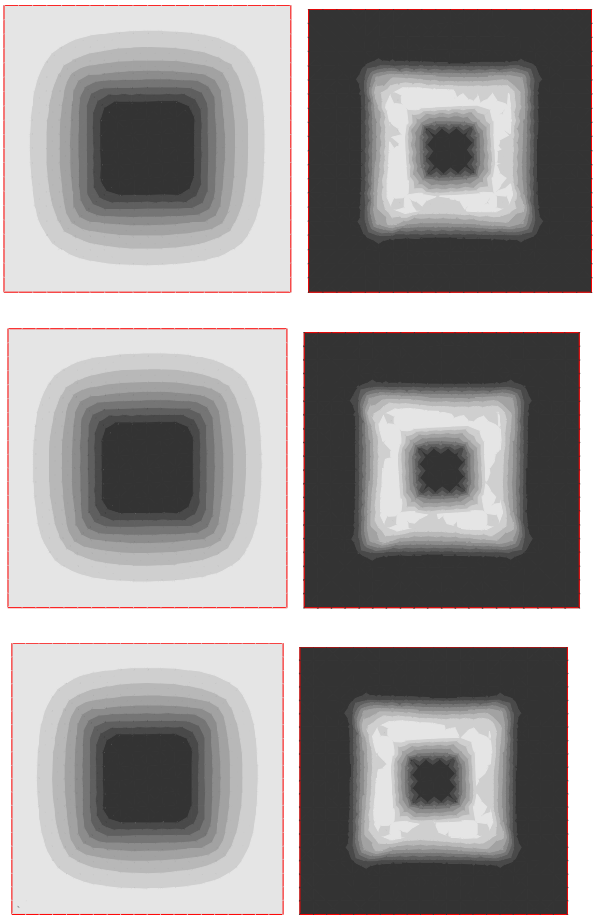

Figure 3: *A comparison of the achieved results: the vertical displacement (left) and the equivalent plastic strain (right) for the standard (top), PLE (middle) and PCLE (bottom).* $S10$ *is used for PLE and PCLE*

4 CONCLUSIONS

In this case study, The PLE and PCLE successfully reduce the computing time required by the Standard method. PLE has a better performance than PCLE. PLE ($S10$) has the highest speed factor of 2.82. A very good agreement of the results are achieved by PLE and PCLE in comparison with the Standard results.

ACKNOWLEDGEMENT

This research was carried out under the project number MC1.05227 in the framework of the Research Program of the Materials innovation institute M2i (www.m2i.nl), the former Netherlands Institute for Metals Research.

REFERENCES

[1] S. Matsubara. Incremental backward bulge forming of a sheet metal with a hemispherical tool. *Journal of the Japan Society for Technology of Plasticity*, 35: 1311–1316, 1994.

[2] M. Bambach, G. Hirt, and J. Ames. Modelling of optimization strategies in the incremental sheet metal forming process. In *NUMIFORM*, pages 1969–1974, 2004.

[3] O. C. Zienkiewicz and R. L. Taylor. *The finite element method for solid and structural mechanics*. Elsevier Butterworth Heinemann, 6th edition, 2005.

[4] G. Hirt, S. Junk, and N. Witulski. Incremental sheet forming: quality evaluation and process simulation. In *7th ICTP Incremental conference on Technology of Plasticity*, pages 925–930, 2002.

[5] T. Belytschko, H. J. Yen, and R. Mullen. Mixed methods in time integration. *Journal of the Japan Society for Technology of Plasticity*, 17-18:259–275, 1979.

[6] T. J. R. Hughes and W. K. Liu. Implicit-explicit finite elements in transient analysis: Implementation an numerical examples. *Journal of Applied mechanics*, 45:375–378, 1978.

[7] B. F. Smith, P. E. Bjorstad, and W. D. Gropp. *Domain decomposition : parallel multilevel methods for elliptic partial differential equations*. Cambridge University Press, 1996.